Update to Proposal E12-06-105

Inclusive Scattering from Nuclei at $x > 1$ in the quasielastic and deeply inelastic regimes

Argonne National Laboratory
University of Virginia
Hampton University
James Madison University
Thomas Jefferson National Accelerator Facility
University of New Hampshire
University of Maryland
University of Tennessee
Yerevan Physics Institute, Armenia

John Arrington, Donal Day, and Nadia Fomin co-spokespersons
(Dated: June 9, 2019)

E12-06-105 was approved to make measurements of inclusive scattering from nuclei at $x > 1$. There are two separate motivations for these measurements, corresponding to two different kinematic regions. Data at moderate Q^2 but very large x ($x > 1.4$) are dominated by quasielastic scattering from extremely high momentum nucleons, and is sensitive to the high-momentum tail of the nucleon distribution in nuclei. The distribution of high momentum nucleons is related to the short range structure and nucleon–nucleon correlations in nuclei. Data at much larger Q^2 for $1 \lesssim x \lesssim 1.5$ are dominated by DIS scattering from the $x \gtrsim 1$ part of the nuclear parton distributions, and can be used to probe the distribution of these exceptionally high momentum quarks. The distribution of these "super-fast quarks" in nuclei is sensitive to short range structure in nuclei, including the possible contribution of non-hadronic components, such as six-quark bags.

This document provides a brief update to and a summary of the original proposal for E12-06-105 [1]. The scientific case for E12-06-105 remains strong and relevant. Precision results from E02-019 and E03-103 [2, 3] showed a suggestive connection between 2N SRCs and the EMC effect. These findings also led to an optimization of the kinematic settings and nuclear target choices to allow us to probe the isospin dependence of both effects. The correlation observed between 2N SRC plateaus as well as the size of the EMC effect has also lead us to coordinate the kinematics and targets with our companion experiment, E12-10-008. An experiment readiness review (ERR) for both efforts was held in 2017, where a final list of targets was approved, but the full experiment has not yet been scheduled.

The current proposal focuses on precision measurements of 2N SRC ratios across nuclei that will allow to further elucidate the nature of the EMC-SRC correlation, first observation of 3N SRCs, and nuclear parton distributions at $x > 1$.

I. INTRODUCTION

Previous measurements of inclusive scattering from nuclei have been made for a range of targets at SLAC [4, 5] and at 4 and 6 GeV at JLAB [2, 6–11]. These 6 GeV Jlab data have yielded some of the most high-impact results from that era, including EMC effect in light nuclei, precision 2N SRC ratios, as well as analyses of the possible relationship between the two. Several measurements have attempted to isolate 3N SRCs [2, 9, 10], but while data are consistent with the presence of 3N SRCs, there is not yet a convincing signal that they have been isolated.

Measurements of A/D cross section ratios can be used to isolate and study the nature of the short range correlations (SRCs) that are the main source of high-momentum nucleons. Precision A/D ratios from 6 GeV data have allowed some studies of the nuclear dependence of 2N SRCs and their connection to the EMC effect, which we aim to continue with focused measurements of this proposal as well as to include studies of isospin dependence. A second plateau at $x > 2$, the expected

signature of 3N SRCs, has not yet been unambiguously observed due to poor resolution [12], low statistics [2], or potentially below threshold kinematics [10]. Recent theoretical work [13, 14] suggests that pushing to higher Q^2 kinematics might be necessary for a definitive observation of a 3N SRC plateau and makes a prediction [14] for the size and A dependence of said plateau. The current kinematics of this proposal (as approved by a 2017 JLab ERR) reflect this fact.

In addition to extending previous measurements of short range correlations, we will provide data at lower x but much higher Q^2 values, where the cross section is dominated by deep inelastic scattering from quarks with $x > 1$. The quark distributions in nuclei at large x are poorly understood, and this will provide the first clean and unambiguous measurement of the distribution of so-called "superfast" quarks. These quark distributions provide an additional way to look for the effect of short range correlations, but also provide high sensitivity to non-hadronic components of nuclear structure in these high density, short range configurations within nuclei [15–17]. Using data from E02-109 we have already had some success in the extraction of the high x structure function distributions [18], as we will discuss below.

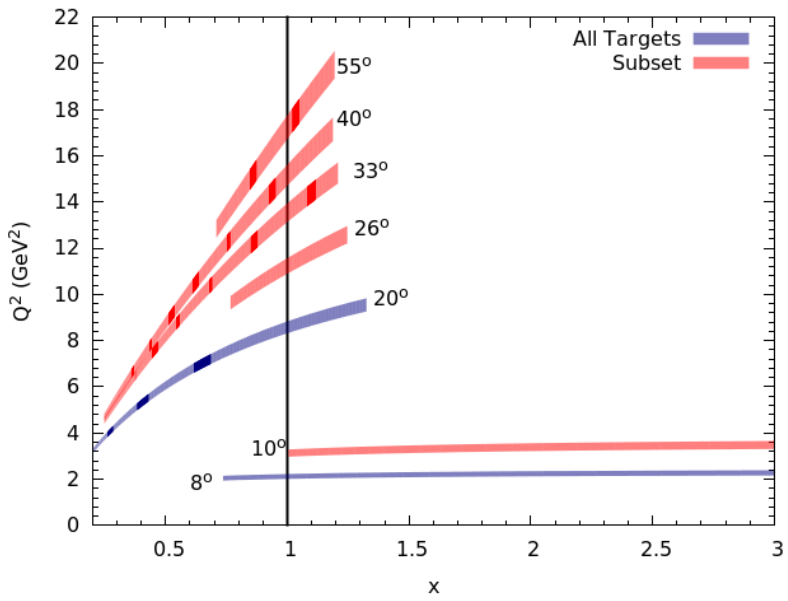

FIG. 1: Kinematic coverage for E12-10-008. The lower x spectrometer settings represent the EMC effect data for E12-10-008, which is expected to run concurrently.

Fig. 1 shows the kinematic coverage for E12-06-105 combined with E12-10-008, which are expected to run concurrently to take advantage of the physics synergy between the two experiments and to map out the SRC/EMC connection for the same nuclei. The selected kinematics aim to address several goals:

- **2N correlations**. The 8°, Q^2 ≈2 GeV^2 setting aims to scan across all target nuclei and obtain precision A/D cross-section rations to study 2N SRCs and their nuclear and isospin dependence as well as the correlation to the EMC effect in DIS. The target list includes a number of light nuclei ($A < 12$) which allow us to examine the impact of clustering effects in SRCs and EMC effect. See Sec. III for details.

- **3N correlations**. The 10°, Q^2 ≈4 GeV^2 setting aims to make the first observation of the

3N scaling plateau. Data on a limited number of targets will be taken, to keep the run times reasonable. See Sec. III for details.

- **Superfast Quarks**. The higher Q^2 data at $x > 1$ aims to probe nuclear parton distributions as well as potential contributions from 6-quark configurations. See Sec. IV.

II. 2N CORRELATIONS AND EMC EFFECT

The 6 GeV era at Jlab has yielded interesting and suggestive results in the form of precision rations of inclusive cross sections for nuclear targets to those of the deuteron (A/D). Scaling was expected in the $x > 1.4$ region, where the electrons scatters from a high-momentum nucleon ($k > 300\ MeV/c$) in the nucleus, with said nucleon originating from a 2N short-range correlation (SRC). The value of the scaling plateau represents the relative number of high-momentum nucleons in A relative to D, modulo center-of-mass motion of the NN pair in the A nucleus. Ratios from E02-019 [2] are shown in the left panel of Fig. 2 with lines corresponding to the fitting regions to extract the plateau value. While the scaling is clear for light nuclei, the shape of the ratio changes for heavier nuclei as the contribution of 3N SRCs begins to show up at high x and the effect of the center-of-mass motion of the NN pair grows (and is known to have an x-dependence).

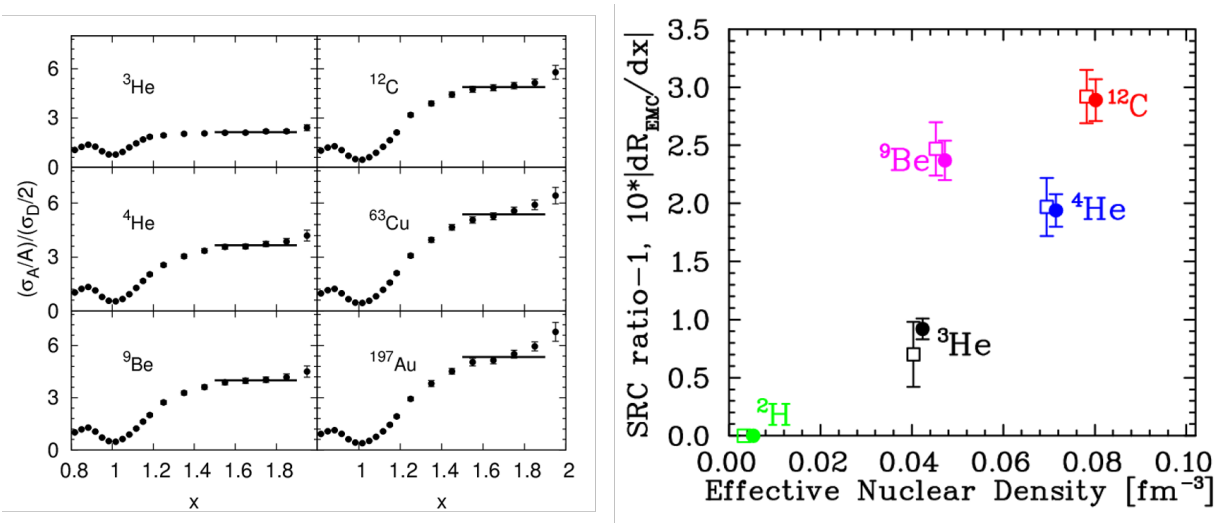

FIG. 2: Left panel: inclusive A/D cross-section ratios, as published by E02-019. Right panel: values of SRC plateaus and EMC effect slopes as a function of effective nuclear density for light nuclei.

Knock-out measurements [19] showed that the 2N SRCs are made-up of predominantly np pairs, raising interesting questions about nuclei with a high neutron excess. Additionally, a precision measurement of the EMC effect light nuclear showed a strikingly similar nuclear dependence to that of 2N SRCs (see right panel of Fig. 2). The EMC effect is an A/D structure function ratio measured in deep inelastic scattering, and the "magnitude" of it refers to the relative depletion of high-x quarks in $A > 2$ nuclei (relative to the deuteron) due to nuclear effects. The exact mechanism that leads to the modification of the nuclear structure function has not been identified in the almost 40 years since its original observation [20], but the strong correlation with the nuclear dependence of 2N SRCs suggests that it may have something to do with short-distance NN pairs (local density, LD) or high-momentum nucleons (high-virtuality, HV). Several analyses [11, 21–23] have examined

this correlation and also tried to extract a universal EMC effect function, but with current data, the results remain inconclusive for now.

To help address these questions, we have updated our target list. ^{9}Be data from the 6 GeV era [2, 3] has yielded interesting results, due to its alpha-like clustering structure, which impacted our understanding of the EMC effect and SRCs. We include additional light nuclei to further flesh out the effect of this nuclear structure. Additionally, we include nuclei with large neutron excess (N/Z ratio) which will allow us to look for isospin dependence, as well as nuclei with similar A, that allow us to scan as a function of N/Z. The targets approved by the ERR are shown in Fig. 3. We believe that the current target list will allow us to separate A dependence and isoscalar dependence, spent for a much cleaner test of isospin dependence.

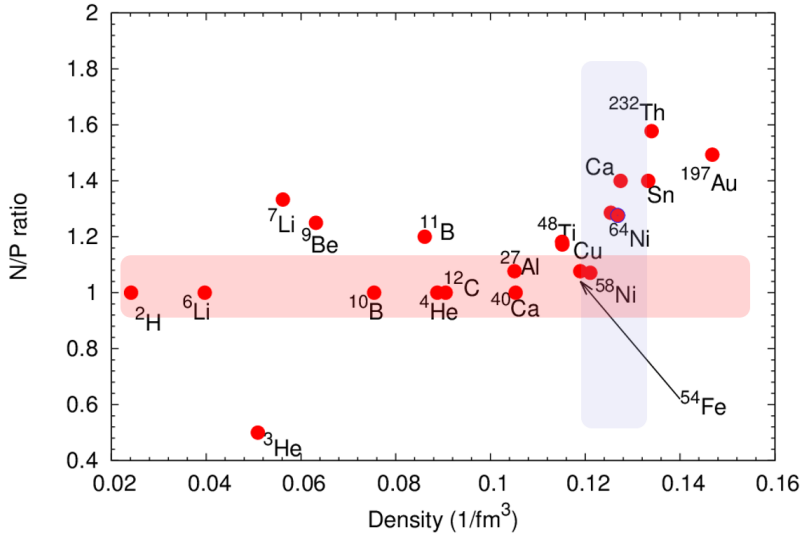

FIG. 3: N/P ratio as a function of nuclear density show for nuclear targets approved by the 2017 ERR for the E12-06-105 and E12-10-008 experiments. Highlighted areas represent scans across isoscalar nuclei (light red) and isospin dependence (light blue).

III. 3N CORRELATIONS

E02-019 aimed to make an observation of a 3N SRC plateau in the $x > 2$ region, but the statistics of the ^{3}He data were insufficient to make a definitive case for 3N SRC dominance. At the same time, the E02-019 results were in tension with the previous CLAS 3N SRC plateau observations [9]. At first, this was potentially ascribed to the different kinematic ranges of the two experiments, but was eventually shown to be an effect of bin migration in the CLAS analysis rather than evidence of 3N SRCs [12]. Jlab E08-014 was approved with the aim of focusing on the $x > 2$ region with longer cryogenic targets (for higher statistics) and a range of kinematics (that overlapped with the CLAS measurements [9]) to map out the onset of a second correlations plateau. None was observed [10] as is illustrated by Fig.4.

Recent work [13, 14] suggests that 3N SRCs do not begin to dominate until much higher Q^2 values. Working in light-cone variables, α_i is analogous to x in QCD and represents the light cone nuclear momentum fraction carried by the constituent nucleon. Just as we define approximate regions in x, where we expect scaling of the A/D cross section ratios, α_i allows for more precise 2N and 3N region

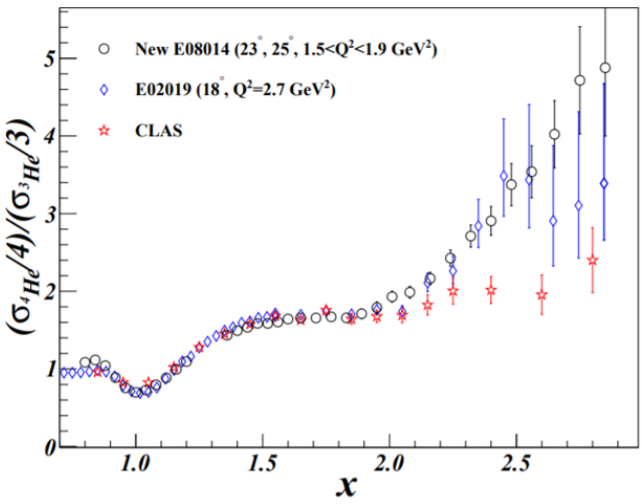

FIG. 4: $A/^3He$ cross section ratios from three Jlab experiments. The higher Q^2 measurements of Hall A and C which are not affected by bin-migration show no evidence of a second, 3N SRC scaling plateau.

isolation. The left panel of Fig. 5 shows α_{3N} for different values of Q^2 as a function of x to show the relationship between the two variables. The authors of Ref. [13, 14] suggest that a minimum of α_{3N}=1.6 - 1.8 is needed to experimentally isolate the second (3N) scaling plateau. The right panel of Fig. 5 illustrates why this is the case by showing calculated contributions from the mean field as well as 2N SRCs, which dominate until α_{3N}=1.6 - 1.8. Both of those need to have sufficiently decayed so that the measured cross section response is dominated by the contributions from 3N SRCs. Note that $\alpha = 1.6$ corresponds to about $x = 2.4$ for E02-019 kinematics. While those ratios (in Fig. 4) are consistent with a plateau, the statistics of the data are insufficient to claim this as significant evidence for a 3N SRC plateau.

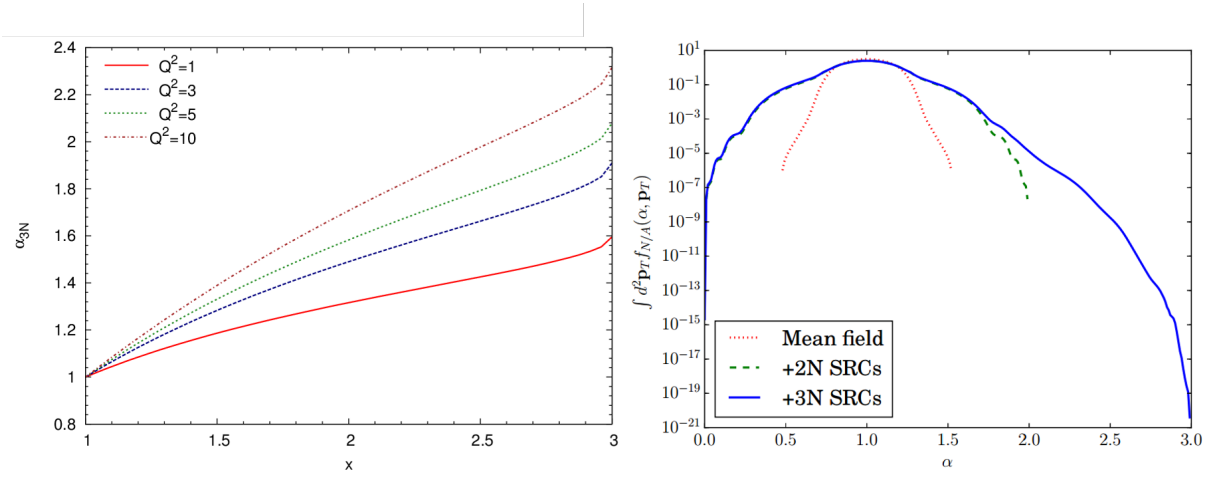

FIG. 5: Left panel shows α_{3N} as a function of x calculated for several values of Q^2. A minimum of α_{3N}=1.6-1.8 is needed to reach a region where 3N SRC contributions dominate, pushing the measurement to a higher Q^2. Right panel [13] shows the different contributions to the measured cross section as a function of α and their decay.

Refs. [13, 14] make a prediction for the probability of finding a nucleon in a 3N SRC, $a_{3N} \sim a_{2N}^2$, assuming that 3N SRCs are predominantly in *ppn* or *nnp* configurations. The authors of Ref [14]

go on to test this hypothesis by assuming scaling in this (α_{3N}=1.6 - 1.8) region, finding that the A dependence of the a_{3N} values is consistent with scaling as a_{2N}^2, in agreement with their model. This suggests that with the current kinematics of this proposal, there is a strong chance of giving a definitive answer to the question of a 3N-SRC scaling plateau.

The proposal has updated the kinematics to reflect this new information. The 10°, ∼4 GeV^2 kinematic setting is aimed at obtaining data on 3N correlations. While precision ratios for 2N SRCs were obtained with $A = 2$ data in the denominator, earlier data using $A/^3He$ ratios [9] exhibited similar plateaus in the $1.4 < x < 1.9$ region as this is where the contribution from 2N SRCs dominates. Analogously, if 3N SRCs can be experimentally observed, they will appear in the $x > 2.5$ region in $A/^3He$ ratios, but will also be seen in $A/^4He$ ratios, which is what we propose to measure. The reason for this is that the region where the 3N scaling plateau is expected to appear is a function of Q^2, growing longer in x with higher Q^2 values as well as an earlier onset in x. At Q^2=4 GeV^2, we expect the onset to occur after x=2.5, which, when combined with the fact that the ^{3}He cross section must fall to zero at x=3, leaves a small region of data for an unambiguous observation. Finally, concerns exist that the motion of the 3N SRC in the $A > 3$ nucleus may have a large impact relative to the stationary ^{3}He nucleus as $x \to 3$, further complicating the interpretation of an $A/^3He$ ratio. For these reasons, we propose to take high statistics data with ^{4}He data to be used in the SRC ratios, and only examine a few additional nuclei as we are looking only for a signature of 3N SRCs.

IV. DEEP INELASTIC SCATTERING AT $x > 1$

The response of the nucleus in the range $x > 1$ is composed of both inelastic scattering from quarks in the nucleus and elastic scattering from the bound nucleons (quasielastic scattering). Previous measurements of electron-nucleus scattering at $x > 1$ have focused on quasielastic scattering, and avoided regions where inelastic contributions have any significant contribution. The increase in energy to 11 GeV will allow us to make measurements at $x > 1$ that are dominated by deeply inelastic scattering, allowing us to and map out the distribution of extremely high momentum nucleons in nuclei.

It has been shown that a better connection can be made between the structure functions and the underlying quark distributions by using the Nachtmann scaling variable, $\xi = 2x/(1 + \sqrt{1 + 4M^2x^2/Q^2})$ [24, 25]. In nuclei, significantly improved scaling is observed at large x when studying the Q^2 dependence of F_2 as a function of ξ rather than x (note that $\xi \to x$ for $Q^2 \to \infty$). These ξ-scaling analyses can be thought of as approximations to the application of target mass corrections, which account for scaling violation at finite Q^2 values. Using the extended kinematic coverage of E02-019, we have performed a more detailed study [18] the scaling of the structure function at large ξ. As a first step we applied the full "target mass" corrections, using the formalism of Ref. [26] to determine $F_2^{(0)}(\xi, Q^2)$, extracted from F_2 using Eq.(23) from Ref. [26]:

$$F_2(x, Q^2) = \frac{x^2}{\xi^2 r^3} F_2^{(0)}(\xi, Q^2) + \frac{6M^2x^3}{Q^2 r^4} h_2(\xi, Q^2) + \frac{12M^4x^4}{Q^4 r^5} g_2(\xi, Q^2), \quad (1)$$

where $h_2(\xi, Q^2) = \int_\xi^A u^{-2} F_2^{(0)}(u, Q^2) du$ and $g_2(\xi, Q^2) = \int_\xi^A v^{-2}(v - \xi) F_2^{(0)}(v, Q^2) dv$.

Calculation of the integrals h_2 and g_2 requires the use of a model for $F_2^{(0)}(\xi, Q^2)$. We make a simple global fit to the world's data at large x and Q^2, to provide a model for calculating h_2 and g_2. This

simple fit provides a reasonable description of the global data set (see Fig. 6), with deviations at low Q^2, in particular near the quasielastic peak ($\xi \approx 0.85$) and for the largest values of ξ. We estimate the model dependence in the extraction of $F_2^{(0)}$ to be $\lesssim$2%.

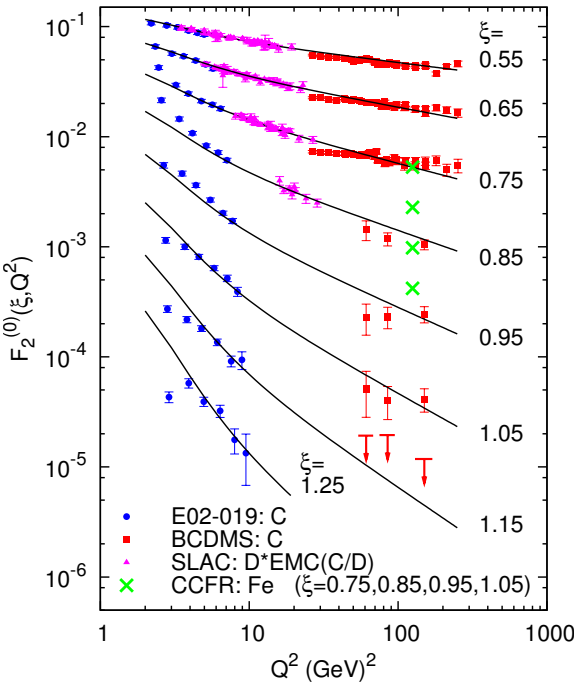

FIG. 6: $F_2^{(0)}$ vs Q^2 for fixed ξ value. For this work and BCDMS, the carbon data are shown, while the SLAC points are carbon pseudo-data taken from measurements on deuterium (see text). The solid curves are the global fit, used to calculate the h_2 and g_2 terms in the target mass corrections. The short horizontal red lines show the BCDMS ξ=1.15 upper limit, and the green crosses show the falloff between ξ=0.75 and ξ=1.05 based on the CCFR data (see text for details).

Figure 6 shows the carbon results for $F_2^{(0)}(\xi, Q^2)$, scaled to fixed values of ξ. For all data sets, $F_2^{(0)}$ is extracted from the measured structure functions using the global fit to calculate g_2 and h_2. The SLAC points are deuterium data [27], multiplied by the SLAC E139 [28] fit to the carbon-to-deuteron structure function ratio, yielding carbon pseudo-data to provide a continuous Q^2 range for lower ξ values. For the lowest ξ value, the three data sets are in good agreement. At low Q^2, the data rise above the global fit in the vicinity of the quasielastic peak ($\xi \approx 0.85$), while at very large ξ values, they fall below the fit. This is consistent with the ξ-scaling observation that the data approach the scaling limit from below as one increases Q^2 [7, 29]. However, the highest Q^2 data from the 6 GeV measurement seem to be consistent with the much higher Q^2 data where it exists, suggesting that even at $Q^2 \approx$ 7–9 GeV^2, the data are consistent with the DIS scaling limit. With the 11 GeV measurement, we will double the Q^2 range, and should be able to extract the quark distributions over a significantly expanded range in ξ.

A. The distribution of superfast quarks

The data from E02-109 has given us a first chance to examine the ξ-dependence of the structure function for large values of ξ and compare to data measured at extremely high Q^2 values ($\sim$ 100 GeV^2) in μ−C scattering [30] and ν-Fe scattering [31]. Near $\xi = 1$, these experiments obtained

significantly different results. The neutrino experiment (CCFR) found $F_2^{Fe} \propto \exp(-8.3x)$ (at these Q^2, the difference between ξ and x is relatively small), consistent with a significant contribution from superfast quarks in the nucleus. The muon experiment (BCDMS) found a much faster falloff $F_2^C \propto \exp(-16.5x)$. The BCDMS data has much lower statistics, while the CCFR experiment has a much poorer resolution in x, and both experiments have limited x coverage, making it difficult to directly compare the results. While the measurements were taken on different nuclei, one would expect the carbon and iron structure functions to be very similar, and a *larger* contribution from superfast quarks for iron, due to the small increase in Fermi momentum.

From the E02-019 data, fit our high Q^2 data for $1 < \xi < 1.25$ to the form $F_2^{(0)} \propto \exp -s\xi$ to compare the falloff to the previous measurements. We obtain $s = 15.0 \pm 0.5$ for carbon, and $s = 14.1 \pm 0.5$ for copper (our closest nucleus to the CCFR iron target). This shows that the large difference between BCDMS and CCFR is not related to the difference in target nuclei, and that the behavior of the structure function at the present Q^2 values is more consistent with the BCDMS result. While the E02-019 results support the conclusions of the BCDMS measurement, they are not a high enough Q^2 to allow for a direct extraction of the nuclear pdfs at $\xi \gtrsim 1$. Because the BCDMS data are limited to $\xi < 1.05$, it is not clear that they have the kinematic reach necessary to test predictions of the high-ξ behavior. In addition, the BCDMS data above $\xi = 0.65$ appear to have little or no Q^2 dependence, which is not consistent with the expectation that there will be significant impact from QCD evolution at large ξ.

B. Sensitivity to Quark Degrees of Freedom in Nuclei

Mapping out the nuclear parton distributions at $x \gtrsim 1$ is not simply a matter of completing our measurements of pdfs in nucleons and nuclei. They also provide important sensitivity to short range structure in nuclei. The quark distribution at $x > 1$ is extremely small in a simple convolution model, as the nucleon quark distributions fall rapidly as $x \to 1$, and there are very few fast nucleons available to boost the quarks to $x > 1$. The bulk of the strength for $x \gtrsim 1.1$–1.2 come from the high momentum nucleons generated by short range correlations in nuclei. In addition, this region is extremely sensitive to the behavior of quarks in nucleons at short range; the number of extremely high momentum quarks can be dramatically increased due to the possibility to directly exchange momentum between the quarks in two nucleons (either through q–q scattering in "overlapping" nucleons or the presence of a small 6-quark bag component).

The EMC effect provides clear evidence that the quark distribution in nuclei is not a simple sum of the quark distributions of it's constituent protons and neutrons. Many explanations of the EMC effect were proposed which involved non-hadronic degrees of freedom in the nucleus, and measurements of the structure functions at $x > 1$ provide a unique sensitivity [16, 17, 32] to such models Figure 7 provides a simple example: It shows the nuclear structure function for deuterium, as calculated from a convolution of neutron and proton structure functions (red), and compares it to the structure function obtained by assuming that 5% of the deuteron wave function is described by a 6-quark bag, using the model of Mulders and Thomas [33] for the quark distribution for the 6-q bag. In the region of the EMC effect ($x < 0.8$), the difference is at most 2%. However, for $x > 1$, the small 6-quark bag component leads to a dramatic increase in the large x parton distributions, due to the free sharing of momentum between the 6 quarks. Note that the 6-quark bag model is taken

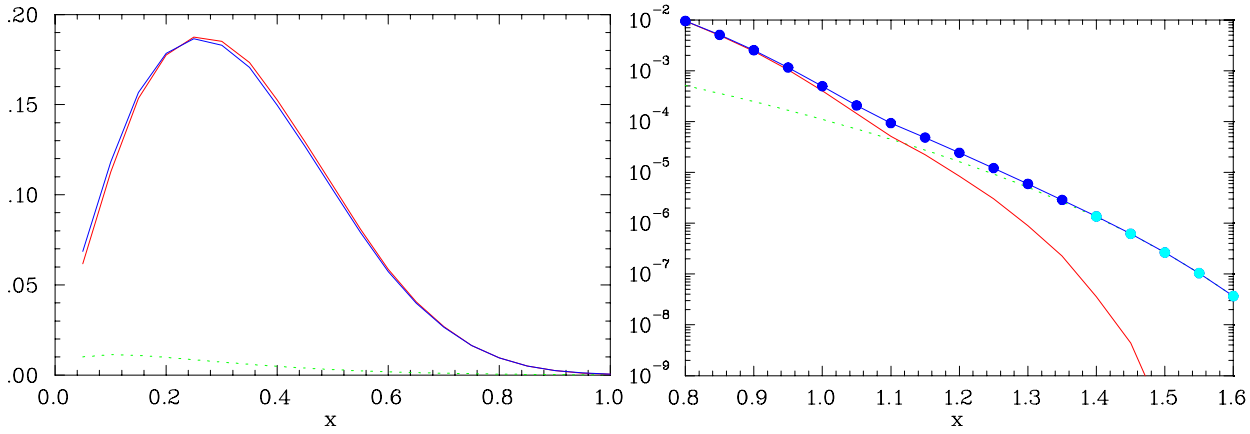

FIG. 7: The deuteron valence quark distributions ($x < 1$ on the left, $x > 1$ on the right) from a convolution of proton and neutron quark distributions (red), and with the inclusions of a 5% 6-quark bag component (blue). The dotted green line shows the contribution from the 6-quark bag component. The circles show projected results for the high Q^2 measurements (the uncertainties are smaller than the points). The points at $x > 1.4$, shown in dark blue, show the region where the cross section is dominated by DIS, although 6 GeV data suggest that precise scaling extends to larger x values.

as a simple model for estimating the impact of an enhanced quark exchange between nucleon with significant wavefunction overlap.

The increase in beam energy to 11 GeV will have the greatest impact on the Q^2 range for kinematic points with $1.0 \lesssim x \lesssim 1.5$. This extended Q^2 data is critical to studies of the extremely large x quark distributions.

V. EXPERIMENTAL EQUIPMENT

The experimental set-up for measurements with a 11 GeV beam would be performed using the existing HMS and SHMS. The HMS would be used for the highest Q^2 measurements at large angles and the SHMS would be used for the intermediate angles, $\lesssim 30^\circ$ providing the intermediate Q^2 measurements for $x \lesssim 1.5$, and the modest Q^2 but very large x measurements.

The target ladder(s) will consist of both cryogenic and thin foil targets. The 2017 ERR has approved the following list: H (calibration), ^{2}H, ^{3,4}He, ^{6,7}Li, ^{9}Be, ^{10,11}B, ^{12}C, ^{27}Al, ^{40,48}Ca,^{48}Ti, ^{54}Fe, ^{58,64}Ni, ^{120}Sn,^{63}Cu, ^{108}Ag, ^{197}Au, and ^{232}Th. As Fig. 1 shows, only two kinematic settings (8° and 20°) will take data with all the nuclear targets for the purposes of mapping out the nuclear dependence of 2N SRCs and nuclear PDFs, and further probing the connection with the EMC effect. The current target list also maximizes sensitivity to isospin effects by varying N/Z while keeping A approximately constant.

No extra beam time is requested due to kinematic setting optimization in concert with E12-10-008 as well as eliminating the third kinematic setting at low Q^2 due to prohibitive runtimes needed to obtain statistically significant results on 3N SRCs.

VI. SUMMARY

We propose to measure inclusive scattering at $x > 1$ on a number of light and heavy nuclei. The carefully chosen nuclear targets will allow us to study the nuclear and isospin dependences

of the 2N SRCs as well as to further scrutinize the SRC/EMC connection. The ability to vary N/Z at approximately constant values of A allows for sensitive and model-independent tests of isospin dependence of both 2N SRCs and EMC effect (which will share the nuclear target list of this experiment). Additionally, measurements of quark distributions at $x > 1$ and high Q^2 provide very different sensitivity to the substructure of the nucleons participating in SRCs, complementing the proposed set of flavor tagged EMC measurements[34–36].

Jlab E12-06-105 promises to provide a wealth of new data on several outstanding physics questions and remains a critical measurement, with its results potentially impacting many other 12 GeV experiments.

[1] J. Arrington and D. Day, Jefferson Lab experiment E12-06-105 (2006).
[2] N. Fomin et al., Phys. Rev. Lett **108**, 092502 (2012).
[3] J. Seely et al., Phys. Rev. Lett. **103**, 202301 (2009).
[4] D. B. Day et al., Phys. Rev. Lett. **43**, 1143 (1979).
[5] D. B. Day et al., Phys. Rev. Lett. **59**, 427 (1987).
[6] J. Arrington et al., Phys. Rev. Lett. **82**, 2056 (1999).
[7] J. Arrington et al., Phys. Rev. C **64**, 014602 (2001).
[8] K. S. Egiyan et al., Phys. Rev. C **68**, 014313 (2003).
[9] K. S. Egiyan et al., Phys. Rev. Lett. **96**, 082501 (2006).
[10] Z. Ye et al. (Hall A), Phys. Rev. **C97**, 065204 (2018), 1712.07009.
[11] B. Schmookler et al., Nature **566**, 354 (2019).
[12] D. W. Higinbotham and O. Hen, Phys. Rev. Lett. **114**, 169201 (2015), 1409.3069.
[13] N. Fomin, D. Higinbotham, M. Sargsian, and P. Solvignon, Ann. Rev. Nucl. Part. Sci. **67**, 129 (2017).
[14] D. B. Day, L. L. Frankfurt, M. M. Sargsian, and M. I. Strikman (2018), submitted to PRL, 1803.07629.
[15] L. L. Frankfurt and M. I. Strikman, Phys. Rept. **160**, 235 (1988).
[16] D. F. Geesaman, K. Saito, and A. W. Thomas, Ann. Rev. Nucl. Sci. **45**, 337 (1995).
[17] M. M. Sargsian et al., J. Phys. **G29**, R1 (2003).
[18] N. Fomin et al., Phys. Rev. Lett. **105**, 212502 (2010), 1008.2713.
[19] R. Subedi et al., Science **320**, 1476 (2008).
[20] J. J. Aubert et al. (European Muon), Phys. Lett. **B105**, 315 (1981).
[21] J. Arrington, A. Daniel, D. Day, N. Fomin, D. Gaskell, and P. Solvignon, Phys. Rev. **C86**, 065204 (2012).
[22] J. Arrington and N. Fomin (2019), 1903.12535.
[23] O. Hen, F. Hauenstein, D. W. Higinbotham, G. A. Miller, E. Piasetzky, A. Schmidt, E. P. Segarra, M. Strikman, and L. B. Weinstein (2019), 1905.02172.
[24] H. Georgi and H. D. Politzer, Phys. Rev. D **14**, 1829 (1976).
[25] O. Nachtmann, Nucl. Phys. **B63**, 237 (1973).
[26] I. Schienbein et al., J. Phys. **G35**, 053101 (2008).
[27] L. W. Whitlow, E. M. Riordan, S. Dasu, S. Rock, and A. Bodek, Phys. Lett. **B282**, 475 (1992).
[28] J. Gomez et al., Phys. Rev. D **49**, 4348 (1994).
[29] B. W. Filippone et al., Phys. Rev. C **45**, 1582 (1992).
[30] A. C. Benvenuti et al. (BCDMS), Phys. Lett. B **189**, 483 (1987).
[31] M. Vakili et al. (CCFR), Phys. Rev. D **61**, 052003 (2000).
[32] M. Arneodo, Phys. Rept. **240**, 301 (1994).
[33] P. J. Mulders and A. W. Thomas, Phys. Rev. Lett. **52**, 1199 (1984).
[34] D. Dutta, D. Gaskell, and K. Hafidi, Jefferson Lab proposal E12-09-004 (2009).
[35] W.-C. Chang, I. Cloet, D. Dutta, and J.-C. Peng, Phys. Lett. **B720**, 188 (2013).
[36] W. Armstrong et al. (2017), jefferson Lab experiment E12-17-012, 1708.00891.